JOURNAL OF MATERIALS SCIENCE 21 (1986) 3501–3508

Pressureless sintering of Si_3N_4 with Y_2O_3 and Al_2O_3

T. HAYASHI, H. MUNAKATA
Department of Applied Chemistry, Faculty of Engineering, Nagoya University, Furo-cho, Chikusa-ku, Nagoya-shi, Aichi-ken 464, Japan

H. SUZUKI, H. SAITO
Department of Mechanical Systems Engineering, Toyota Technological Institute, 2-12-1, Hisakata, Tenpaku-ku, Nagoya-shi, Aichi-ken 468, Japan

Pressureless sintering of Si_3N_4 with Y_2O_3 and Al_2O_3 as additives was carried out at 1750° C in N_2 atmosphere. Si_3N_4 materials which had more than 92% relative density were obtained with 20 wt% addition of additives. The flexural strength of as-sintered materials containing 5 to 8.6 wt% Al_2O_3 and 15 to 11.4 wt% Y_2O_3 was in the range of 480 to 560 MPa at room temperature. The glassy grain-boundary phase of as-sintered materials crystallized to $3Y_2O_3 \cdot 5Al_2O_3$ (YAG), $Y_2O_3 \cdot SiO_2$ (YS), $Y_2O_3 \cdot 2SiO_2$ (Y2S) and $10Y_2O_3 \cdot 9SiO_2 \cdot Si_3N_4$ (NA) by heat-treatment at 1250° C for 3 days. A specimen containing 15 wt% Y_2O_3 and 5 wt% Al_2O_3 sintered at 1750° C for 4 h was heat-treated at 1250° C for 3 days to precipitate YAG and YS. The nitrogen concentration of the grain-boundary glassy phase of the specimen was found to be very high, and therefore the flexural strength of the crystallized specimen scarcely decreased at elevated temperatures (the flexural strength of this specimen is 390 MPa at room temperature and 360 MPa at 1300° C). Resistance to oxidation at 1200° C of the specimen was good as well as the flexural strength, compared with that of as-sintered materials.

1. Introduction

Silicon nitride is one of the promising candidates for heat engines capable of operating in the temperature range from 1300 to 1400° C, because of its excellent high-temperature mechanical properties, resistance to oxidation and thermal shock.

However, it is difficult to densify Si_3N_4 without using metal oxides as additives. Since these metal oxides ultimately form a grain-boundary glassy phase which degrades the high-temperature mechanical properties of sintered materials, the following methods have been used to solve this problem; (i) hot-pressing and hot isostatic pressing of Si_3N_4 containing a lesser amount of additives compared with pressureless sintering [1–3], and (ii) crystallization of grain-boundary glassy phase in the range 1100 to 1400° C in N_2 atmosphere after pressureless sintering of Si_3N_4 with additives [4–7]. But Method (i) has several problems such as higher cost of sintering, a difficulty of preparing complicated materials, etc. Accordingly, Method (ii) is desirable for industrial materials.

Pressureless sintering is carried out up to 1800° C because Si_3N_4 decomposes at about 1800° C and above 1700° C the surface silica on Si_3N_4 particles may be considered as an additive because it becomes vitreous. However, it reacts with Si_3N_4 to form an oxynitride before its viscosity can become low enough to assist in the sintering process. Y_2O_3 is a commonly used additive, and the reaction between SiO_2, Y_2O_3 and Si_3N_4 produces a liquid phase able to bring about densification with $\alpha \rightarrow \beta$ transformation. Y_2O_3 improves the strength of sintered materials because the liquid formed during sintering reacts further with Si_3N_4 to produce a refractory grain-boundary phase. The addition of Al_2O_3 to Si_3N_4 containing Y_2O_3 was more effective to assist in the sintering process. Rowcliffe and Jorgensen [8] showed that amorphous Si_3N_4 powder with Y_2O_3 and Al_2O_3 could be sintered to a relative density of more than 95%. The sintering kinetics in this system have been reported by Leohman and Rowcliffe [9] and by Jack [10]. In this work, pressureless sintering of Si_3N_4 with Y_2O_3 and Al_2O_3 as additives was carried out and the crystallization of grain-boundary glassy phase of as-sintered materials was performed to improve the high-temperature mechanical properties.

2. Experimental procedure

2.1. Materials

Si_3N_4 powder was supplied by Herman C. Stark (Berlin); Y_2O_3 (99.99% pure) and Al_2O_3 (98.8% pure) were supplied by Wako Pure Chemical Industries (Osaka, Japan) and Kanto Chemical Co. (Tokyo, Japan), respectively. Table I gives the chemical analysis of Si_3N_4 powder.

2.2. Sintering

Si_3N_4, Y_2O_3 and Al_2O_3 were mixed in isopropyl alcohol in an automatic agate mortar for 2 h. The amount of additive was 10 or 20 wt %. Compositions of the additives are shown in Fig. 1. The mixed powder was weighed out (about 3 g) and then uniaxially

0022–2461/86 $03.00 + .12

TABLE I Chemical analysis of as-received Si_3N_4 powder

Phase (%)	Average particle size (μm)	Impurities (wt %)					
		Free Si	Fe	Al	Ca	O	C
α (88) β (10)	0.7	< 0.1	0.04	0.1	0.03	1.3	0.4

pressed at 147 MPa. The size of the green compacts was 40 mm × 8 mm × 4 mm. The green compacts were dried at 100 and 400° C, and then sintered at 1750° C in N_2 atmosphere. Powder beds were used to suppress the decomposition of Si_3N_4 at high temperature.

2.3. Properties

Weight loss, linear shrinkage, bulk density and three-point bending strength of sintered materials were measured. The size of specimens for bending tests was 25 mm × 5 mm × 3 mm and the specimens were finally polished using 0.05 μm Al_2O_3. A scanning electron microscope (SEM) was available to observe fractographs of sintered materials.

2.4. Crystallization of grain-boundary glassy phase

The crystallization of grain-boundary glassy phase was performed to improve the high-temperature mechanical properties of as-sintered materials. Specimens were embedded in a powder of composition $40Si_3N_4$–40BN–20 (additives) (wt %) and heat-treated at 1000, 1250 and 1400° C in N_2 atmosphere. The crystalline phases precipitated by heat-treatment of sintered materials were identified by X-ray powder diffraction.

The bulk density and flexural strength of specimens at room and elevated temperatures were measured by the Archimedes method and three-point bending method, respectively. Fracture surfaces of specimens fractured at room and elevated temperatures were observed by SEM. The resistance to oxidation at elevated temperature was also examined by measuring the weight gain of crystallized specimens after heat-treatment at 1200° C in air.

3. Results and discussion

3.1. Additives and powder bed compositions

The density, linear shrinkage, weight loss and flexural strength at room temperature of materials sintered at 1750° C for 1.5 h in N_2 atmosphere were measured and the result is shown in Table II. 20 wt % addition was found to be more effective for pressureless sintering than 10 wt % addition. Sintered Si_3N_4 materials which had a flexural strength of more than 480 MPa at room temperature and a bulk density of more than 3.10 g cm^{-3} were obtained in the case of No. 2, No. 3 ($Y_2O_3 \cdot Al_2O_3$) and No. 4 (YAG) additives. Fig. 1 shows the glass-forming region of the system Si_3N_4–SiO_2–Y_2O_3–Al_2O_3. It is well known that the sinterability of Si_3N_4 is influenced by the liquid phase formed by the reaction of Si_3N_4 with additives. As shown in Fig. 1 and Table II, the compositions of additives which gave Si_3N_4 materials having relatively high bulk density and flexural strength were those lying in the glass-forming region, although the content of Si_3N_4 in the grain-boundary glassy phase was not determined. This suggested that the formation of stable liquid phases was necessary for the liquid-phase sintering of Si_3N_4.

Moreover, it was important to decrease the extent of decomposition of Si_3N_4 and secondary glassy phases in order to obtain dense Si_3N_4 materials by pressureless sintering. For this purpose, a powder bed technique was used in this work. Mitomo *et al.* [11] showed that it was possible to prepare β-Sialon having more than 95% relative density by the sintering of Si_3N_4 under 10 atm N_2 pressure. Pompe and Carlsson [12] showed the protective effect of the powder bed technique. Also, Gazza *et al.* [13] succeeded in obtaining fully dense Si_3N_4 materials by a dual N_2 pressure process. The role of N_2 pressure has also been reported by Greskovich and Prochazka [14]. The decomposition of phases containing oxides occurs according to the following equations (where M = metal):

$$Si_3N_4(s) + 3SiO_2(s) \rightarrow 6SiO(g) + 2N_2(g)$$

$$3Si_2N_2O(s) \rightarrow Si_3N_4(s) + 3SiO(g) + N_2(g)$$

$$Si_3N_4(s) + 3MO(s) \rightarrow 3M(g) + 3SiO(g) + 2N_2(g)$$

$$Si_3N_4(s) \rightarrow 3Si(g) + 2N_2(g)$$

$$(Si–M–O–N)\ \text{glass} \rightarrow SiO(g) + N_2(g) + (\text{M-containing solids})$$

The decomposition reactions might occur in the presence of carbon. As green compacts were sintered in a graphite vessel in this work, the effect of compositions of powder bed on the sinterability was examined by the sintering of Si_3N_4 with No. 4 additive and the results are shown in Table III. In the case of Si_3N_4, BN or $50Si_3N_4$–50BN (wt %) as a powder bed, weight loss during sintering occurred considerably, and sintered Si_3N_4 materials became heterogeneous near the

TABLE II Properties of as-sintered Si_3N_4 materials sintered at 1750° C for 1.5 h in Si_3N_4 powder

No.	Composition (wt %)			Weight loss (%)	$\Delta L/L_0$ (%)	Bulk density (g cm^{-3})	Percentage of theoretical density	Strength (MPa)
	Si_3N_4	Y_2O_3	Al_2O_3					
1	90	8.2	1.9	3.0	6	2.43	75	235
	80	16.3	3.7	2.0	13	2.98	89	314
2	80	15	5.0	3.8	16	3.11	92	480
3	80	13.8	6.2	3.0	16	3.18	94	490
4	90	5.7	4.3	6.9	11	2.62	89	314
	80	11.4	8.6	3.0	15	3.10	92	500
5	80	9	11.0	2.6	14	3.09	94	392
6	80	6.5	13.5	3.3	13	3.00	92	402

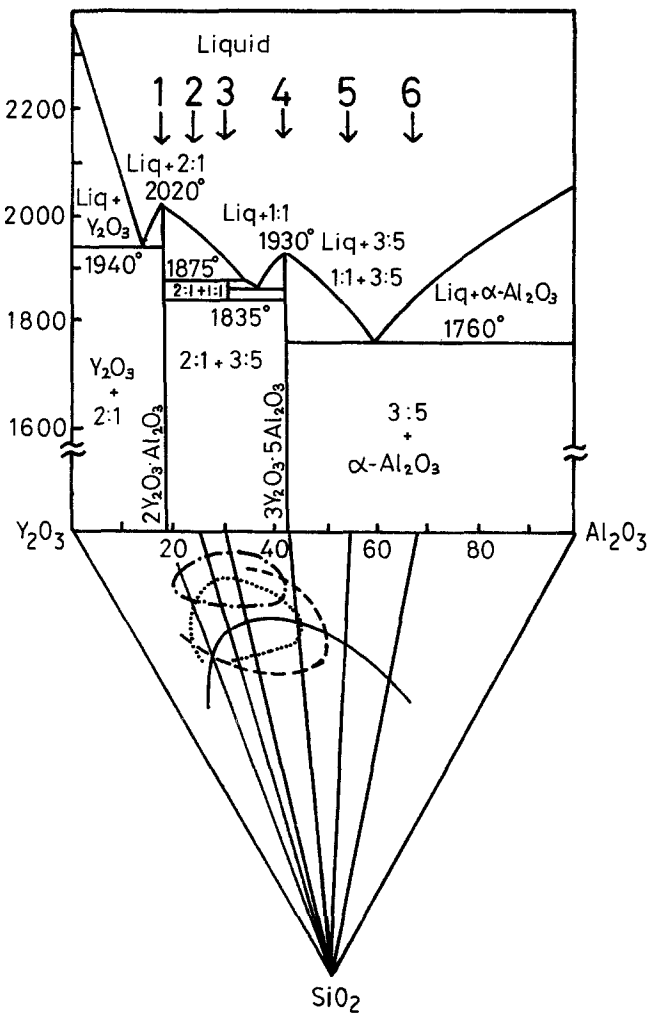

Figure 1 Glass-forming region in the system Si_3N_4–Y_2O_3–Al_2O_3–SiO_2. Nitrogen content (eq %) as follows: (——) 0, (– – –) 14, (- - -) 20, (– - –) 25.

surface. On the other hand, when $70Si_3N_4$–$30SiO_2$ powder was used, weight loss scarcely occurred because the decomposition of Si_3N_4 and secondary glassy phases was restrained during sintering by SiO vapour formed from the powder bed, according to the following equations:

$$Si_3N_4 + SiO_2 \rightarrow 2Si_2N_2O$$

$$3Si_2N_2O \rightarrow Si_3N_4 + 3SiO + N_2$$

In practice, Si_2N_2O was detected in the powder bed after sintering. However, the sinterability was not good in this case. The reason for this could not be clarified, but excess SiO might prevent the sintering process. The optimum composition of a powder bed was found to be $40Si_3N_4$–40BN–20 (additives) because the decomposition of Si_3N_4 and secondary glassy phase were greatly suppressed at high temperature.

3.2. The sintering process

Pressureless sintering of Si_3N_4 with No. 2, No. 3 or No. 4 additives embedded in $40Si_3N_4$–40BN–20 (additives) powder was carried out at 1750° C in N_2 atmosphere. The results of sintering for 1.5 h are shown in Table IV. With No. 2 and No. 3 additives, the flexural strengths of sintered materials at room temperature were more than 510 MPa. In this case, the weight loss decreased, and both the bulk density and flexural strength increased, compared with specimens sintered in Si_3N_4 powder bed (see Table II).

The change of properties of as-sintered materials containing No. 2 additive ($15Y_2O_3$–$5Al_2O_3$) with sintering time is shown in Fig. 2. Prolonged sintering was possible for pressureless sintering of Si_3N_4 by the powder bed technique because the decomposition of Si_3N_4 materials was restrained during sintering. As a result, Si_3N_4 materials which had 98% relative density (bulk density = 3.33 g cm^{-3}) was obtained by

TABLE III Effects of powder bed composition

Powder bed composition (wt %)	Weight loss (%)	$\Delta L/L_0$ (%)	Bulk density (g cm^{-3})	Percentage of theoretical density	Strength (MPa)
Si_3N_4	2.5	14	3.18	94	490
BN	3.8	15	3.18	94	–
$50Si_3N_4$–50BN	0.8	15	3.18	94	–
$70Si_3N_4$–$30SiO_2$	0.3	12	2.94	87	382
$80Si_3N_4$–20 (additives)	1.5	15	3.19	94	421
$40Si_3N_4$–40BN–20 (additives)	1.0	15	3.19	94	421

TABLE IV Properties of as-sintered Si_3N_4 materials, sintered at 1750° C for 1.5 h

No.	Powder bed composition (wt%)	Weight loss (%)	$\Delta L/L_0$ (%)	Bulk density ($g\,cm^{-3}$)	Percentage of theoretical density	Strength (MPa)
2	$40Si_3N_4$–40BN–20 (additives)	0.9	15	3.22	95	559
3	$40Si_3N_4$–40BN–20 (additives)	1.0	15	3.22	95	510
4	$40Si_3N_4$–40BN–20 (additives)	1.0	15	3.19	94	421

pressureless sintering at 1750° C for 4 h. The microstructure of this specimen is shown in Fig. 3. Elongated β-Si_3N_4 grains were observed and its interlocking structure was developed with further sintering. The grain growth seemed to proceed at prolonged sintering time. Whether dense Si_3N_4 materials could be obtainable or not by pressureless sintering depended upon the formation of a suitable amount of liquid phase which was stable and viscous, and had a high solubility of Si_3N_4 at sintering temperatures. It was possible to prepare fully dense Si_3N_4 materials by pressureless sintering of green compacts embedded in a suitable powder.

It is well known that the sintering of Si_3N_4 with additives occurs by a liquid-phase mechanism in which the kinetics exhibit three stages predicted by Kingery's model [10]. Log (linear shrinkage) against log (sintering time) plots for the sintering of Si_3N_4 are shown in Fig. 4. For elongated grains, the relative shrinkage during the second or solution-precipitation stage can be described by the equation

$$(\Delta L/L_0) = (\Delta V/3V_0) = (At)^{1/n}$$

where t is time and A is a constant; $n = 3$ or $n = 5$ according to whether the phase-boundary reaction or diffusion is rate-limiting. In this work $n = 5$, suggesting diffusion through the liquid phase, was obtained in the solution-precipitation stage. This might be attributed to the high viscosity of the liquid phase in the system Si_3N_4–SiO_2–Al_2O_3–Y_2O_3 which was formed during sintering. A considerable amount of residual glassy phase, which led to a decrease of the flexural strength at elevated temperature, existed in the grain boundaries of sintered materials. Hence, the crystallization of the residual glassy phase was necessary to improve high-temperature strength.

3.3. Crystallization of grain-boundary glassy phase

The strength of pressureless-sintered Si_3N_4 materials decreased at elevated temperature because of the presence of either low-melting eutectic or glassy phases at the grain boundaries. The improvement of high-temperature mechanical properties of Si_3N_4 materials by crystallization was reported by Tsuge *et al.* [6]. Sintered Si_3N_4 materials with Y_2O_3 and Al_2O_3 as additives was heat-treated to crystallize the grain-boundary glassy phase and precipitate $Y_2O_3 \cdot Si_3N_4$, which are highly refractory. By the heat-treatment, Si_3N_4 materials with excellent high-temperature mechanical properties were obtained.

However, it is important to consider the properties of crystallized phases for the improvement of mechanical properties of Si_3N_4 materials. For example, if the thermal expansion coefficients of crystallized phases mismatch with that of Si_3N_4, microcracks arise in the grain boundaries of sintered materials at a moderate temperature and the flexural strength decreases.

Crystallization temperatures were determined from differential thermal analysis (DTA) curves. DTA curves of Si_3N_4 materials sintered with No. 2, No. 3 or No. 4 additive are shown in Fig. 5. Exothermic peaks were observed in all samples both at 980 to 1000° C and at 1225 to 1290° C. The former peak and the latter peak were due to the precipitation of unknown phase, and YAG and Y2S, respectively.

Since exothermic peaks of DTA curves and precipitated phases corresponding to the peaks were similar to those of oxynitride glasses obtained in other work [15], it was assumed that the composition of the grain-boundary phases resembled those of oxynitride glasses of composition $8.0Si_3N_4$–$19.5SiO_2$–$30.5Al_2O_3$–$42.0Y_2O_3$ (wt %). Thus, heat-treatment was done at 1000, 1250 and 1400° C. Table V shows the precipitated phases of specimens crystallized at 1000, 1250 and 1400° C. An unknown phase (UK) precipitated from the secondary glassy phase by heat-treatment around 1000° C for more than 3 days, and the amount precipitated reached a constant by heat-treatment at 1250° C for more than 1 day. YAG and YS were crystallized as major phases at 1250° C and YN was crystallized at 1400° C.

The effect of heating time at 1250° C on the crystallization of grain-boundary phases was studied and the results are shown in Fig. 6. In the initial stage, the relative amount of unknown phase increased appreciably with the heating time, but began to decrease around 10 h heating. Thereafter YAG was formed along with the decrease of the unknown phase and its amount increased with the heating time, and then the curves level off around 3 days. Therefore, the crystallization was carried out at 1250° C for 3 days.

The bulk density and flexural strength of crystallized specimens are shown in Table VI. The flexural strength at room temperature decreased after the

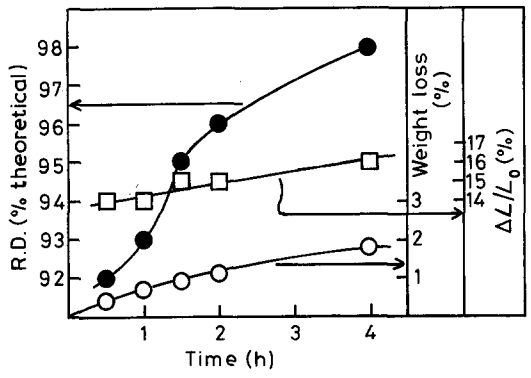

Figure 2 Relationship between sintering time and properties of as-sintered Si_3N_4 materials, sintered at 1750° C. R.D. = relative density.

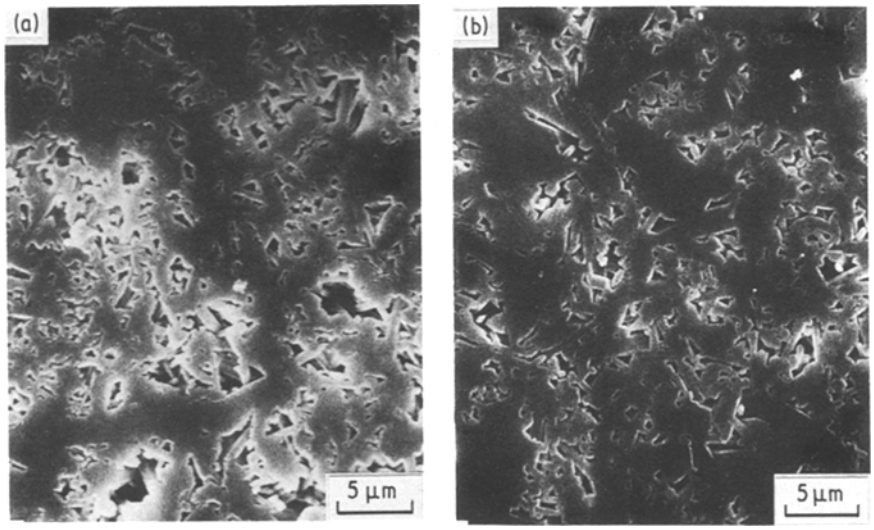

Figure 3 Scanning electron micrographs of as-sintered (Si_3N_4 + 20 wt % No. 2 additive) polished surface: (A) sintered 1750° C–1.5 h, (B) sintered 1750° C–4 h.

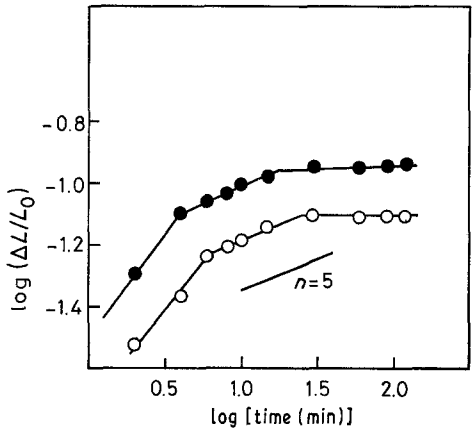

Figure 4 Relationship between sintering time and linear shrinkage of Si_3N_4 materials sintered at 1700° C: (○) Si_3N_4 + 20 wt % No. 1 additive, (●) Si_3N_4 + 20 wt % No. 4 additive.

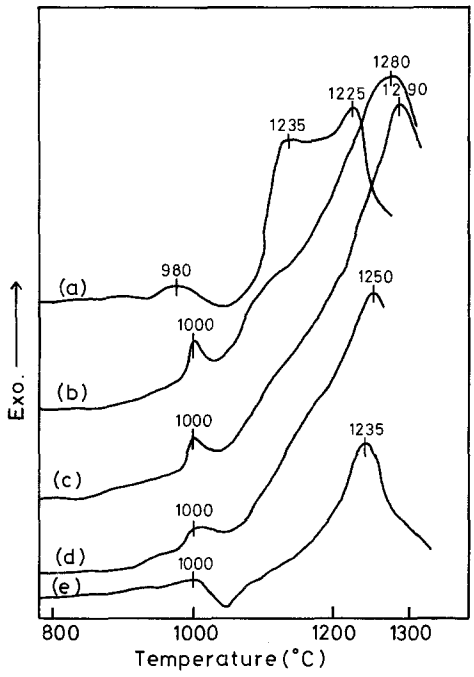

Figure 5 DTA curves of as-sintered Si_3N_4 materials and oxynitride glasses: (a) glass $7.5Si_3N_4$–$24.3SiO_2$–$16.2Al_2O_3$–$52.0Y_2O_3$ (wt %), (b) Si_3N_4 + 20 wt % No. 2 additive, (c) Si_3N_4 + 20 wt % No. 3 additive, (d) Si_3N_4 + 20 wt % No. 4 additive, (e) glass $8.0Si_3N_4$–$19.5SiO_2$–$30.5Al_2O_3$–$42.0Y_2O_3$ (wt %).

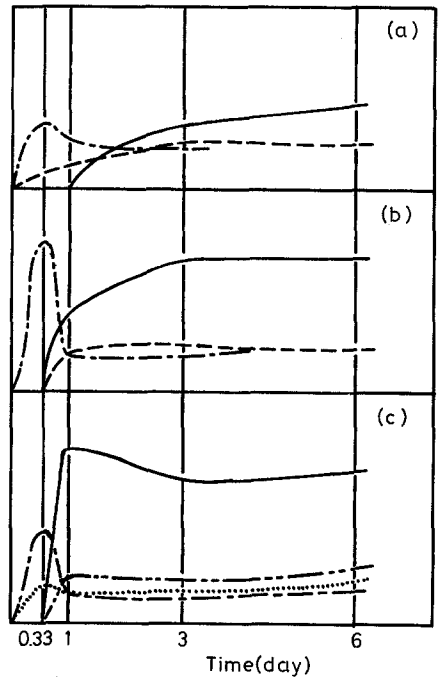

Figure 6 Change of the amount (plotted in arbitrary units) of crystalline phases precipitated by heat-treatment at 1250° C with heating time: (——) YAG, (– – –) YS, (– – –) UK, (– – –) Y2S, (- - -) N-apatite. (a) Si_3N_4 + 20 wt % No. 2 additive, (b) Si_3N_4 + 20 wt % No. 3 additive, (c) Si_3N_4 + 20 wt % No. 4 additive.

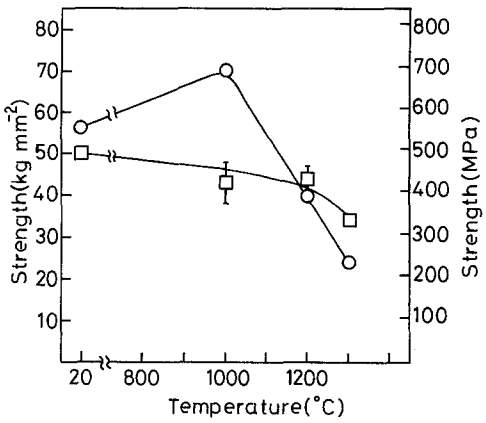

Figure 7 High-temperature flexural strength of Si_3N_4 + 20 wt % No. 2 additive: (○) as-sintered, 1750° C–2 h; (□) crystallized, 1250° C–3 days.

TABLE V Crystalline phases precipitated after heat-treatment*

No.	As-sintered	1000° C–6 days	1250° C–3 days	1400° C–8 h
2	β	β, UK	β, YAG, YS	β, YN, YAG, YS
3	β	β, UK	β, YAG, YS	β, YN, YAG, YS
4	β	β, UK	β, YAG, YS, Y2S, NA	β, NM, YAG, YN

*β = β-Si_3N_4, YAG = $3Y_2O_3 \cdot 5Al_2O_3$, YS = $Y_2O_3 \cdot SiO_2$, YN = $YSiO_2N$, Y2S = $Y_2O_3 \cdot 2SiO_2$, NM = $Y_2O_3 \cdot Si_3N_4$, NA = $10Y_2O_3 \cdot 9SiO_2 \cdot Si_3N_4$, UK = unknown.

crystallization because of the change of specific volume of grain-boundary phases and the difference of thermal expansion coefficients between Si_3N_4 and crystallized phases. The flexural strength at elevated temperature is shown in Figs 7 and 8. Flexural strengths of as-sintered materials increased at 1000° C (Fig. 7). This may be due to the blusting of flows existing on the Si_3N_4 materials by the oxide scale formed during the bending test. At 1200° C, the flexural strengths of crystallized specimens were higher than those of as-sintered materials. This tendency was remarkable at 1300° C.

Fracture surfaces of as-sintered and crystallized (Si_3N_4 + 20 wt % No. 2 additive) materials are shown in Figs 9 and 10, respectively. In as-sintered Si_3N_4 materials, the fracture seemed to occur in the Si_3N_4 matrix below 1000° C and in the glassy grain boundaries at or above 1200° C, while in crystallized specimens the fractures occurred predominantly at grain boundaries above the crystallization temperature, i.e. 1250° C, and in the Si_3N_4 matrix below the crystallization temperature. The degradation of high-temperature mechanical properties began at 1300° C in the crystallized specimens and at about 1200°C in as-sintered materials. The flexural strength of crystallized specimens was maintained at a value as high as 360 MPa at 1300° C. These results showed that the crystallization was very effective in improving high-temperature mechanical properties.

In this system, the reaction of Y_2O_3 with Si_3N_4 to form nitrogen melilite, which slowly disappeared with increasing heating time, might occur in the initial stage. Extensive work on oxynitride glasses has shown that Si_3N_4 dissolves in molten SiO_2–Y_2O_3–Al_2O_3 above 1550° C and forms a liquid phase which can be quenched to oxynitride glasses containing up to 9 at % nitrogen [16]. Also, Leohman and Rowcliffe [9] showed that in this system, the amorphous grain-boundary phase contained about 6 at % nitrogen. But in this work, nitride compounds were not precipitated in the specimens crystallized at 1250° C and only oxide compounds were precipitated. Therefore, nitrogen in the residual glassy phase increases with the precipitation of oxide compounds from oxynitride glass, resulting in an increase of the softening point of the glassy phase. Further, DTA curves of oxynitride glasses containing 6 at % nitrogen were found to be similar to those of sintered Si_3N_4 materials. Consequently, an improvement of the flexural strength could be attained by decreasing the amount of grain-boundary glassy phase and increasing the N_2 concentration of the residual glassy phase.

Resistance to oxidation was also measured. The weight gain of crystallized specimens by heat-treatment at elevated temperature was measured and is shown in Fig. 11. The oxidation reaction occurred according to the equation

$$Si_3N_4 + 3O_2 \rightarrow 3SiO_2 + 2N_2$$

In accordance with the mechanical properties, the resistance to oxidation increased by heat-treatment at 1250° C while it decreased by heat-treatment at 1400° C because of the precipitated oxynitride phases, such as $YSiO_2N$. The oxidation behaviour seemed to obey a parabolic law.

TABLE VI Effects of heat-treatment at 1250° C for 3 days

No.	Composition (wt %)			Bulk density ($g\,cm^{-3}$)*	Strength (MPa)*
	Si_3N_4	Y_2O_3	Al_2O_3		
2	80	15	5	3.23(3.22) (3.33)†	490(560) 392(510)†
3	80	13.8	6.2	3.24(3.22)	353(510)
4	80	11.4	8.6	3.15(3.19)	343(421)

*( ) as-sintered, 1750° C–1.5 h; ( )† as-sintered, 1750° C–4 h.

4. Conclusions

Sintered Si_3N_4 materials of which the flexural strength was more than 480 MPa were obtained by pressureless sintering at 1750° C in N_2 atmosphere. The crystallization of as-sintered materials was carried out to improve the high-temperature mechanical properties. The flexural strength of crystallized specimens hardly decreased up to 1300° C and was about 360 MPa at 1300° C.

An improvement of the resistance to oxidation was

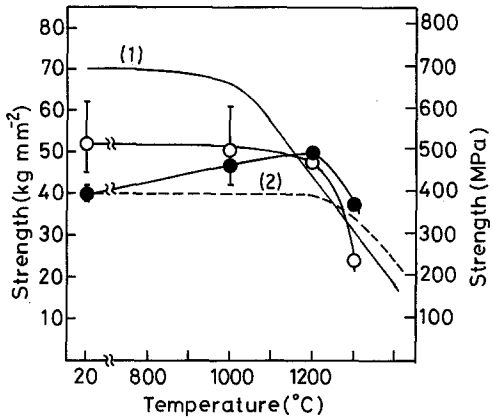

Figure 8 High-temperature flexural strengths of Si_3N_4 materials. Experimental points for Si_3N_4 + 20 wt % No. 2 additive, (○) as-sintered, 1750° C–4 h; (●) crystallized, 1250° C–3 days. Data also given for (——) (1) (Si_3N_4 + 6 wt % Y_2O_3 + 1.5 wt % Al_2O_3) (Smith and Quackenbush [17]), (– – –) (2) β-Sialon (Mitomo *et al.* [18]).

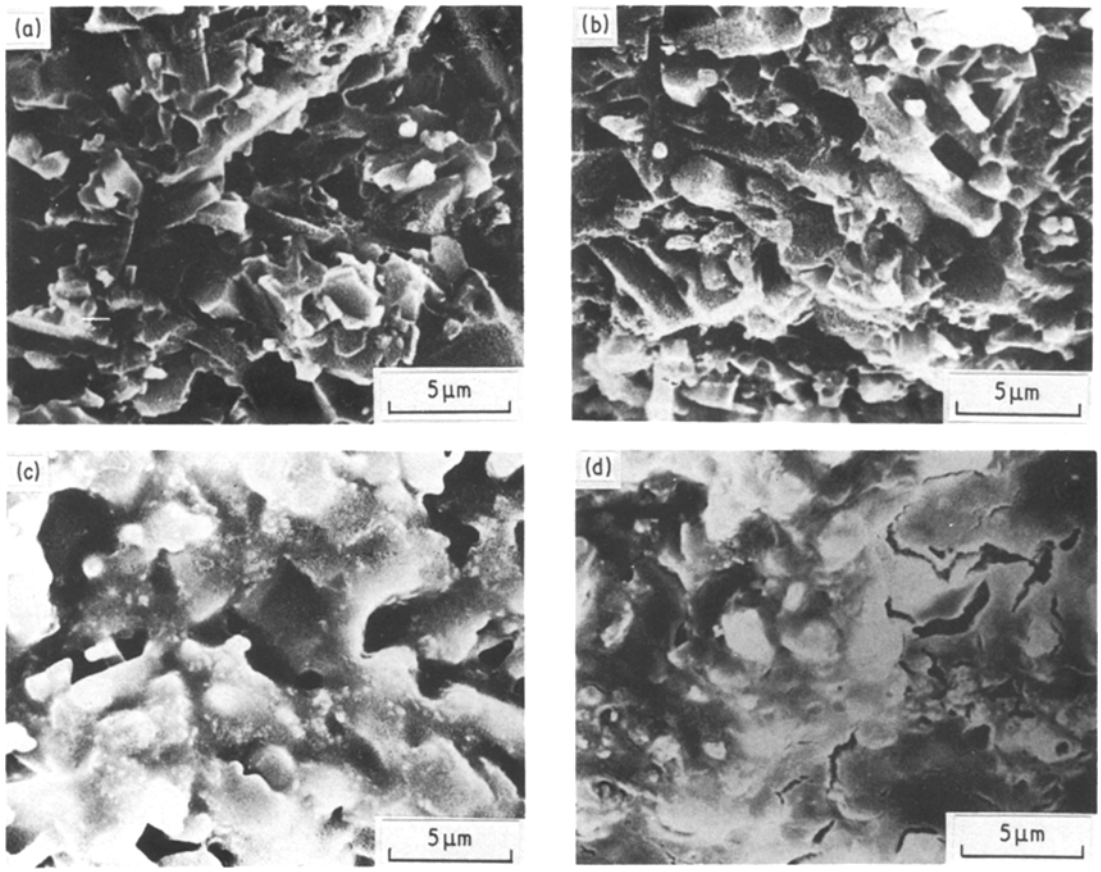

Figure 9 Scanning electron micrographs of as-sintered Si_3N_4 + 20 wt % No. 2 additive fracture surfaces: (a) fractured at room temperature, (b) fractured at 1000° C, (c) fractured at 1200° C, (d) fractured at 1300° C.

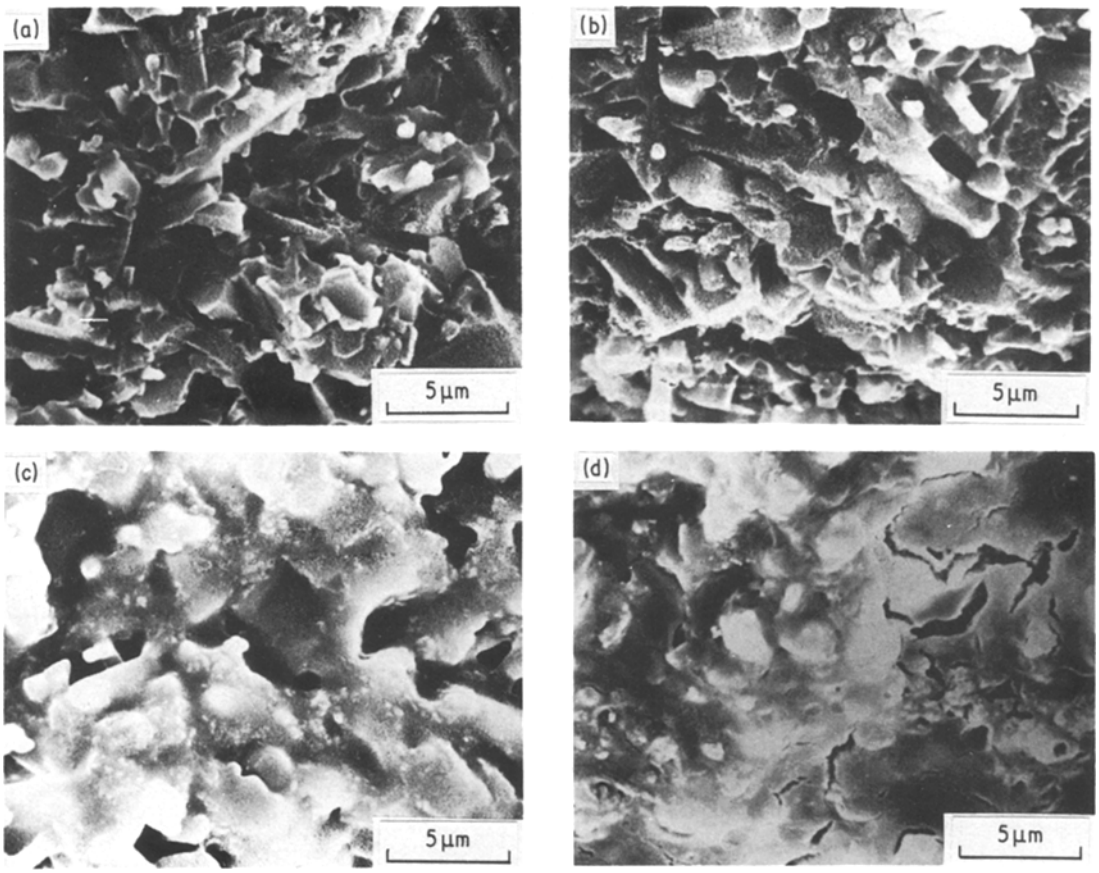

Figure 10 Scanning electron micrographs of crystallized Si_3N_4 + 20 wt % No. 2 additive fracture surfaces: (a) fractured at room temperature, (b) fractured at 1000° C, (c) fractured at 1200° C, (d) fractured at 1300° C.

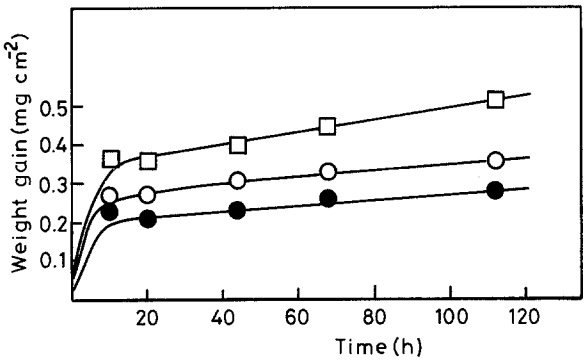

Figure 11 Resistance to oxidation of Si_3N_4 + 20 wt % No. 2 additive in air: (○) as-sintered, (●) crystallized, 1250° C–3 days, (□) crystallized, 1400° C–8 h.

also attained by the crystallization of as-sintered materials. The improvement of high-temperature mechanical properties of crystallized Si_3N_4 materials might be due to the decrease of the amount of grain-boundary glassy phase and the increase of N_2 concentration in the residual glassy phase, which gave rise to an increase of the softening point of the glassy phase.

In this work, crystallization of the grain-boundary glassy phase was found to be very effective in improving the high-temperature properties of Si_3N_4 materials.

References

1. O. YEHESKEL, Y. GEFEN and M. TALIANKER, *J. Mater. Sci.* **19** (1984) 745.
2. K. HIROTA, T. ICHIKIZAKI, Y. HASEGAWA and H. SUZUKI, in Proceedings of the First International Symposium on Ceramic Components for Engines, Japan, edited by S. Somiya, E. Kanai and K. Ando, Hakone, Japan, 17–19 October (1983) p. 434.
3. S. SOMIYA, M. YOSHIMURA, S. FUJIWARA, A. SAWANO and K. KONDO, *ibid.*, p. 442.
4. P. GREIL, J. C. BRESSIANI and G. PETZOW, *ibid.*, p. 228.
5. H. R. ZHUANG, W. L. LI, D. Q. HUA, S. L. WEN, Y. Y. SUN, X. R. FU and T. S. YEN, *ibid.*, p. 368.
6. A. TSUGE, K. NISHIDA and M. KOMATSU, *J. Amer. Ceram. Soc.* **58** (1975) 323.
7. A. TSUGE and K. NISHIDA, *Amer. Ceram. Soc. Bull.* **57** (1978) 424.
8. D. J. ROWCLIFFE and P. J. JORGENSEN, SRI International Final Technical Report, NSF Grant No. AER 75-14896 (1977).
9. R. E. LEOHMAN and D. J. ROWCLIFFE, *J. Amer. Ceram. Soc.* **63** (1980) 144.
10. P. VINCENZINI, "Energy and Ceramics" (Elsevier, 1980) p. 534.
11. M. MITOMO, N. KURAMOTO and Y. INOMATA, *J. Mater. Sci.* **14** (1979) 2309.
12. R. POMPE and R. CARLSSON, "Progress in Nitrogen Ceramics", edited by F. L. Riley (Martinus Nijhoff, The Hague, 1983) p. 219.
13. G. E. GAZZA, R. N. KATZ and H. F. PRIEST, *J. Amer. Ceram. Soc.* **64** (1981) C-161.
14. C. GRESKOVICH and S. PROCHAZKA, *ibid.* **64** (1981) C-96.
15. T. HAYASHI, unpublished work.
16. R. E. LEOHMAN, *J. Amer. Ceram. Soc.* **62** (1979) 491.
17. J. THOMAS SMITH and C. LANE QUACKENBUSH, *Amer. Ceram. Soc. Bull.* **59** (1980) 529.
18. M. MITOMO, N. KURAMOTO, Y. INOMATA and M. TSUTSUMI, *Yogyo-Kyokai-Shi* **88** (1980) 489.

Received 17 October
and accepted 9 December 1985